RESEARCH ARTICLE

Fatigue muscle strength estimation model for athletes based on electromyographic signals

Zhiyong Wang*

Henan University of Urban Construction, Pingdingshan, Henan, China.

Received: January 22, 2024; **accepted:** March 15, 2024.

In order to provide a method to accurately predict the fatigue level of athletes, this study proposed a fatigue muscle strength estimation model for athletes based on electromyography signals. The model achieved prediction of the electromyography-muscle force relationship by continuously generating new solutions and sorting and updating them according to the cost function in order to find the optimal model parameters. The experimental data showed that the low and high frequency components of electromyography signals were effectively removed after band-pass filtering at 50 - 300 Hz, resulting in clearer and more accurate signals. The mean frequency and median frequency showed a high negative correlation with fatigue severity with correlation coefficients of -0.766 and -0.663, respectively. Compared to the classical polynomial fitting model, the error of the Laguerre-Volterra network feature-weighted local sparsity correction model was reduced by approximately 5%, and the model fit was improved by approximately 21%. The results showed that the fatigue strength estimation model based on electromyography signals could accurately predict the fatigue level of athletes, which could provide an important basis for optimizing athletes' training plans and improving athletic performance.

Keywords: electromyography; athletes; fatigue muscle strength; time domain features; frequency domain features.

***Corresponding author:** Zhiyong Wang, Henan University of Urban Construction, Pingdingshan 467036, Henan, China. Emails: wangzhiyong0375@163.com.

Introduction

Fatigue is one of the common problems faced by athletes during prolonged high-intensity training or competition [1]. Understanding the level of fatigue in athletes is important for optimizing training programs and improving competitive performance. As the level of competitive sports continues to improve, it has become increasingly important for athletes to recognize and manage fatigue [2]. Currently, there are many methods to assess the level of fatigue in athletes including heart rate variability, blood biochemical indicators, psychological questionnaires, *etc*. [3]. However, these methods often require complex equipment and specialized personnel, limiting their application in practical training scenarios. Electromyography (EMG) is a bioelectrical signal that records muscle activity, which can reflect the contraction and relaxation state of muscles and is therefore widely used in the fields of exercise physiology and rehabilitation medicine [4]. In recent years, more and more studies have shown that there is a correlation between EMG signals and the degree of fatigue, and therefore, it can be used to estimate the fatigue muscle strength of athletes. The non-invasive, real-time nature of EMG signals and their direct correlation with muscle activity make them an ideal fatigue monitoring tool [5]. EMG is a technique for recording and analyzing the electrical activity of muscle cells by means of electrodes or stimulation of the skin surface, and can be used to assess muscle fatigue, nerve injuries, and the diagnosis and treatment of motor and neurological disorders. Moissenet *et al*. evaluated the effect of two different normalization tasks for the rectus femoris muscle on the quality of the EMG signals, as well as the diurnal and interlay ratings of the amplitude of the EMG signals under both intra- and inter-day rating reliability tasks. The results showed that the signal-to-noise ratio was greater than 15 dB for the two different normalizations tasks [6]. Dideriksen *et al*. investigated the correlation between synaptic inputs to the motor neuron pool and muscle force including different synaptic command signal bandwidths and muscle contraction characteristics. The results showed that cumulative spike training to estimate the entropy of descending muscle force commands could better reflect the sequential behavioral changes [7]. Wang *et al*. proposed the strategy of using cell-free materials for muscle damage repair and predicted muscle atrophy by EMG signal acquisition. The results showed that the maximum contraction force of denervated muscles was restored by 50% after muscle damage repair [8]. Takenaka *et al*. used motor imagery in a reaction-time task paradigm and measured EMG changes associated with muscle contraction and relaxation and found that the excitability of contraction and diastolic motor imagery showed a sustained increase, a transient increase, and a subsequent decrease in excitability, respectively [9]. Tang *et al*. used time-delayed neural network mapping to classify muscle movements and control an external hardware device by controlling the EMG. The results showed that the maximum average classification rate of the model was 91.09% and 91.55% for reference power features and frequency band power features, respectively [10].

Human fatigue state estimation refers to the use of various methods and techniques to determine and assess the degree of fatigue of the human body during a specific task or exercise. This estimation can be achieved by monitoring and analyzing physiological and psychological indicators of the human body. Li *et al*. assessed the changes in muscle state during fatigue using image entropy by capturing static sustained contraction parameters of the biceps muscle at four different intensities of the athletes. The results showed a gradual increase in the root mean square value of surface EMG during sustained contraction [11]. Rakshit *et al*. found that the Three Compartment Controller (3CC-r) muscle fatigue model could predict the performance of both sustained and intermittent isometric contractions through a comprehensive validation of the model. The results showed that the prediction error of the model could be reduced by 8% after considering the effects of functional muscle groups and gender [12]. Wang *et al*. proposed a driving fatigue detection method based on phase lag exponential graphical attention network (PLI-GAT), which used PLI to construct a functional brain network reflecting the relationship between different channels of EEG signals and to model the multichannel time-frequency features as graphical data using GAT to train the driving fatigue monitoring model. The results showed that the accuracy of this method for fatigue state recognition reached 85.53% [13]. Kim *et al*. investigated the use of ultrasound speckle tracking to assess muscle contractility and built a dynamic model to determine and update the optimal inputs to the neuromuscular system in real time. Experiments demonstrated that peak strain and maximum knee torque during isometric knee extension of the quadriceps muscle measured by ultrasound imaging could reflect the strain field and fatigue level correlations of the target muscle [14]. Villanueva *et al*. proposed an improved model-based approach to quantify subjective fatigue accrued from mid-air interactions, which additionally captured the maximum arm posture-based arm strength and added model parameters based on linear changes in current muscle strength. The results showed that the model was able to reduce the fatigue estimation error by 42.5% compared to previous methods [15].

Many researchers have done different studies and designs for EMG and fatigue estimation. However, the scope of application of these methods and models still needs to be improved. Relatively few studies have been conducted on fatigue muscle force estimation models for athletes based on EMG signals. Therefore, the aim of this study was to explore the relationship between EMG signals and athletes' fatigue muscle strength and to establish a reliable estimation model based on electromyography signals, which could accurately predict the degree of athlete fatigue and provide important basis for optimizing athlete training plans and improving sports performance.

Materials and methods

Research subjects

This study recruited 20 college student volunteers including 10 males and 10 females and all aged 25. The volunteers had no history of muscle related illnesses, and all came from the same university in Beijing, China. The testing was conducted at the university's gymnasium. The EMG was acquired from each participant with a sampling frequency of 1,950 Hz by using EMG100C Ultrium EMG high precision EMG signal collector (BIOPAC Systems, Inc., Goleta, CA, USA). All procedures were approved by the university Ethics Committee (Beijing, China).

EMG signal data acquisition and processing

The time-domain features of EMG include waveform, amplitude, frequency, phase, *etc.*, which reflect the changing process and characteristics of muscle electrical activity [16]. The waveform length of EMG time-domain features was calculated below.

$$\begin{cases} WL = \sum_{i=1}^{N-1} \left| x_{i+1} - x_i \right| \\ DAWV = \dfrac{\sum_{i=1}^{N-1} \left| x_{i+1} - x_i \right|}{N-1} \end{cases} \quad (1)$$

where *WL* was the waveform length. *N* was the number of samples. x_i was the value of the i th sample. *DAWV* was the difference absolute mean value of signal. The calculation of muscle activity intensity was shown in equation (2).

$$IEMG = \sum_{i=1}^{N} \left| x_i \right| \quad (2)$$

where *IEMG* was the integration of absolute of EMG signal value. The muscle contraction point correlation was calculated as below.

$$\begin{cases} MAV = \dfrac{\sum_{i=1}^{N} \left| x_i \right|}{N} \\ MAVS = MAV(i+1) - MAV(i) \end{cases} \quad (3)$$

where *MAV* was the mean absolute value of amplitude. *MAVS* was the mean absolute value slope of signal. The EMG average energy value and signal strength were calculated below.

$$\begin{cases} RMS = \sqrt{\sum_{i=1}^{N} \left| x_i \right|^2 / N} \\ VAR = \dfrac{1}{N-1} \sum_{i=1}^{N} \left| x_i \right|^2 \end{cases} \quad (4)$$

where *RMS* was the root mean square of EMG. *VAR* was the variance of signal. Meanwhile, zero crossing (ZC) was the number of times the EMG waveform changes at the zero point, which reflected the synchronization and stability of the muscle electrical activity. Wilson amplitude of signal (WAMP) was the difference between the maximum amplitude and the minimum amplitude of the signal, which was used to describe the degree of amplitude change of the signal, the larger the amplitude change, the larger the WAMP value. Simple square integral of signal (SSI) was the sum of the squared values of the signal over a period of time, which was used to describe the energy characteristics of the signal, the greater the energy, the greater the SSI value. Slope-sign change (SSC) was the number

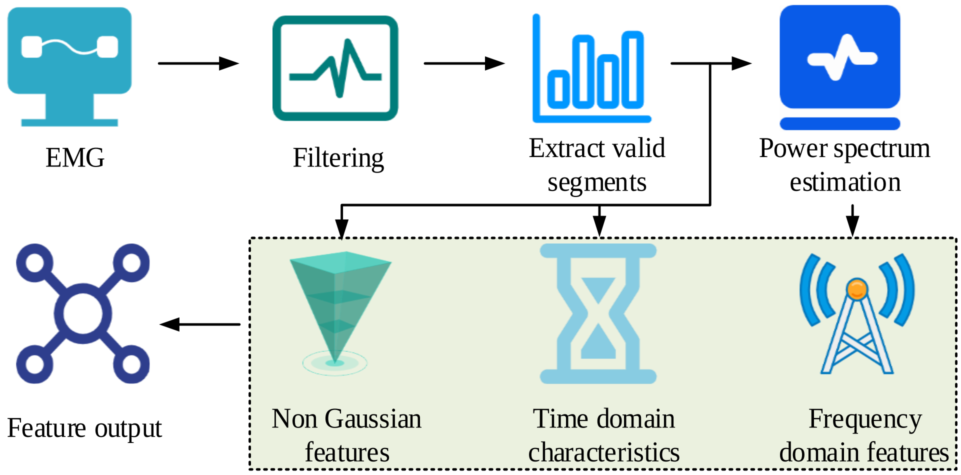

Figure 1. EMG feature extraction method.

of changes in the slope of the signal in the time domain, which was used to describe the rate of change of the signal [17, 18]. The frequency domain characteristics of the EMG were the characteristics of the signal in the frequency domain, and the peak frequency was calculated as shown in equation (5).

$$PF = f(\max_i(p_1, p_2, \ldots, p_N)) \quad (5)$$

where PF was the peak frequency. p_i was the power spectral intensity corresponding to the frequency f_i. The frequency domain features of EMG also included the mean frequency (MPF), total power (TP), median frequency (MDF), mean instantaneous frequency (MIF), and fatigue index based on spectral moment (FI). The non-Gaussian features of EMG referred to the fact that the electrical signals generated by muscle activity did not statistically conform to a Gaussian distribution, i.e., their probability density functions did not exhibit the typical bell curve shape, and its measurement parameters contained crag and negentropy [19, 20]. In order to analyze the characteristic changes of EMG in different fatigue stages, the study convened volunteers for EMG acquisition. The EMG feature extraction method was shown in Figure 1. Since the acquisition of EMG signals was often subject to various interferences such as electromyographic noise and signal interference, the signals needed to be denoised before feature extraction and computation. In order to remove the high frequency and low frequency noise in the original EMG, band-pass filtering was selected for the study. In EMG signals, different parts of muscles produced different electrical signals during movement. Therefore, active segment extraction of the signals was needed to extract site-specific muscle activity information [21]. Common active segment extraction methods include threshold-based methods, frequency domain-based methods, *etc.*, which can be selected according to different application scenarios. Power spectrum estimation is a method that transfers the signal energy to the frequency domain, which can extract the muscle activity information at different frequencies. Through power spectrum estimation, the frequency distribution of muscle activity can be more accurately understood [22]. Correlation feature calculation is a method to correlate multiple signals, which can extract the correlation information between different signals. Common correlation feature calculation methods include Pearson correlation coefficient, Spearman rank correlation coefficient, and so on. By correlation feature calculation, the relationship between different signals can be understood more accurately [23]. The EMG feature analysis method was shown in Figure 2.

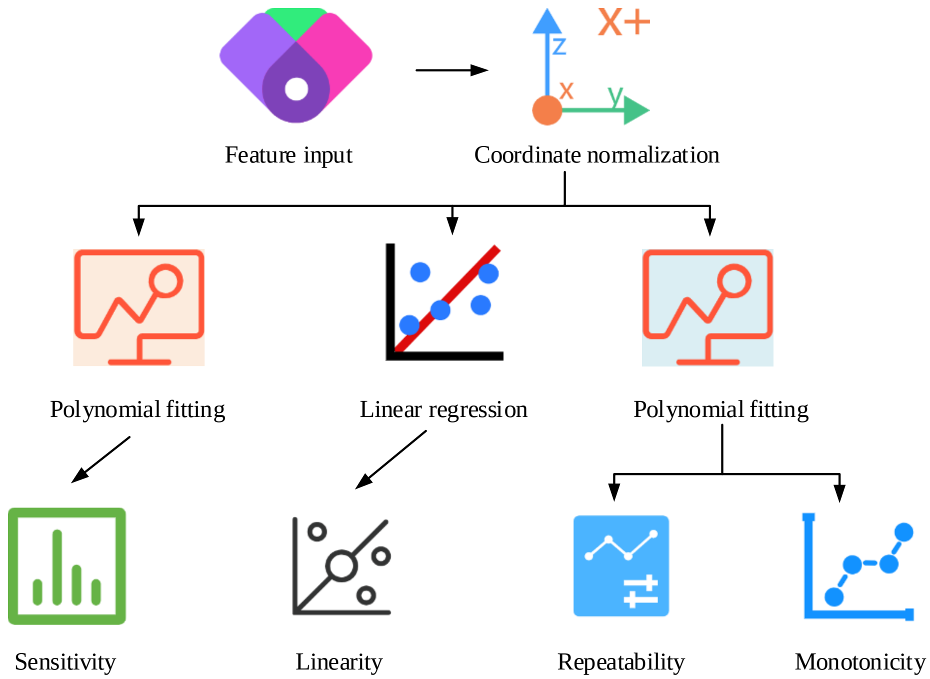

Figure 2. EMG feature analysis method.

EMG signature analysis methods can quantitatively and qualitatively analyze the characteristic information of EMG. Qualitative analysis is to analyze EMG signals by observing and judging the morphology, amplitude, frequency, and other features of EMG signals, which mainly relies on manual experience and polynomial fitting to judge the activity state of muscles such as muscle contraction, relaxation, fatigue, *etc*. by observing the waveform, amplitude, duration, and other features of EMG. Quantitative analysis is to analyze EMG through mathematical and statistical methods to obtain specific numerical results, which mainly relies on computers and related software to process and analyze EMG. The relationship between related features and fatigue level was analyzed by fitting the characteristic parameters of EMG signals such as mean, variance, power spectral density, *etc*. The effective segment of EMG was normalized as below.

$$\bar{I} = \frac{I}{FN} \times 100\% \qquad (6)$$

where *I* was the effective segment. *FN* was the total number of segments. $\bar{I}$ was the normalized effective segment. The feature parameter normalization was shown in equation (7).

$$\bar{F}(i) = \frac{F(i) - F_{\min}}{F_{\max} - F_{\min}} \qquad (7)$$

Where *F(i)* was the i th eigenvalue. F_{max} was the maximum eigenvalue. F_{min} was the minimum eigenvalue. $\bar{F}(i)$ was the normalized i th eigenvalue. The correlation between EMG features and fatigue changes was shown in equation (8).

$$PF = \frac{\sum_{i=1}^{N}(F(i) - \bar{F}(i))(I - \bar{I})}{\sqrt{\sum_{i=1}^{N}(F(i) - \bar{F}(i))^2 \sum_{i=1}^{N}(I - \bar{I})^2}} \qquad (8)$$

where *PF* was the Pearson correlation coefficient. Its positive or negative indicated that

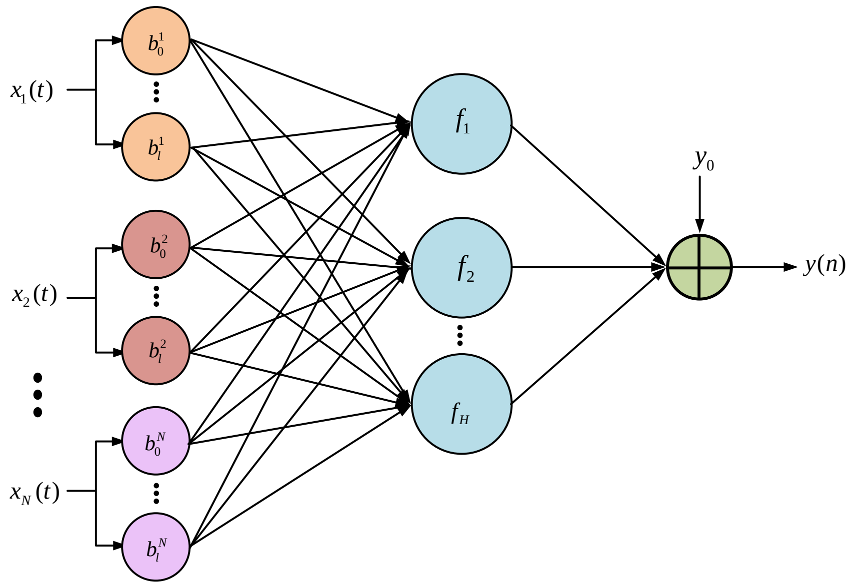

Figure 3. Multi input LVN model.

the EMG features showed positive or negative correlation with fatigue. The sensitivity of the change of features with fatigue was calculated as shown in equation (9).

$$CFS = \frac{\max(SOF) - \min(SOF)}{\sqrt{\frac{1}{N}\sum_{i=1}^{N}(F(i) - SOF(i))^2}} \tag{9}$$

where *CFS* was the feature fatigue sensitivity, whose larger value indicated that the feature was more actively affected by fatigue. *SOF* was the second order fitted eigenvalue.

Model design for estimating fatigue muscle strength in athletes

In electromyography-muscle force modelling, the Laguerre-Volterra network (LVN) was used to simulate the interactions between muscles and the nervous system [24]. Each node in the model represented a muscle fiber, and the connections between the nodes represented the coordination and regulatory relationships between the muscle fibers. By simulating synaptic transmission between neurons and force transmission between muscle fibers, the model could predict the relationship between EMG signals and muscle force. The single-input LVN model had some drawbacks in simulating the EMG-muscle force relationship including the inability to simulate multi-muscle coordinated movements and the inability to accurately simulate the non-linear properties and fatigue effects of muscles. Therefore, the study extended the LVN inputs. The multi-input LVN model was shown in Figure 3.

The output of the input signal processed by the filter bank was the convolution of the input with the Laguerre function. The output of the filter bank was shown in equation (10).

$$v_{jn}^{n}(t) = T\sum_{m=0}^{M-1} b_{jn}(m)x_n(t-m) \tag{10}$$

where *N* was the number of input signals. l was the number of Laguerre function $b_{jn}(m)$. *T* was the length of data points. *M* was the length of memory. The output of the multi-input LVN model $y(t)$ was shown in equation (11).

$$y(t) = y_0 + \sum_{h=1}^{H} z_h(t) \tag{11}$$

where H was the number of the second layer outputs $z_h(t)$ of the multi-input LVN model. y_0 was the output of the single-output LVN model. The inputs of the single input LVN model were shown in equation (12).

$$x_{LVN\_1} = \bar{\sigma} \tag{12}$$

where x_{LVN_1} was the input to the single input LVN model. $\bar{\sigma}$ was the mean EMG standard deviation. The input to the weighted fusion feature model was shown in equation (13).

$$x_{LVN\_S} = W_{fea} \times Fea \tag{13}$$

where x_{LVN_S} was the input of the weighted fusion feature model. W_{fea} was the feature weights. *Fea* was the fatigue feature matrix. The local sparse cost of the weighted fusion feature model was calculated below.

$$J_{LVN\_S} = NMSE + \lambda \sum_{i=1}^{Q} |w_i| \tag{14}$$

where J_{LVN_S} was the local sparsity cost. *NMSE* was the normalized mean square error. $\lambda \sum_{i=1}^{Q} |w_i|$ was the local sparsity penalty term. λ was the penalty strength coefficient. Q and w_i were the numbers of features and weights, respectively.

In order to reduce the time of model training, the study guided the search direction of the continuous domain ant colony algorithm by updating the global optimal solution, so that it was more likely to find the global optimal solution. At the same time, the global update mechanism could also increase the diversity of the algorithm and avoid the ants from falling into the situation of local optimal solutions. The LVN feature-weighted local sparsity correction model (LVN-FS) training process included initializing the parameters and calculating all possible sampling values, initializing the continuous domain ant colony parameters and calculating the weights of the solution combinations, initializing the solution archive SOL by forwarding propagation and solving the LVN model determined by the combination, and then calculating the intermediate and estimated outputs of the LVN model. SOL was sorted in ascending order according to the cost function. In each iteration, the guide solution index was determined based on the probability and a new solution was generated based on the guide solution. Then forward propagation was performed and the intermediate and estimated outputs of the LVN model were calculated based on the LVN model determined from the new solution. The new solutions were ranked according to the cost function. The new and old solutions were combined and sorted in ascending order according to the cost function as a new SOL. A global update was performed to generate a uniform sampling value between 0 and 1. When it was less than 0.9, a new solution was constructed by using the solutions in the SOL in order as the guide solution. The first solution combination of the new SOL was used as the optimal solution combination for the current loop. The steps were repeated until the maximum number of iterations was reached. The solution combination parameters were shown as follows.

$$[\beta_1, \beta_2, y_0, C, W_1, W_2, W_{fea}] \tag{15}$$

where β1 and β2 were the uniformly sampled values. C, W_1, W_2 were matrices with different number of rows and same number of columns, respectively.

The fatigue muscle strength estimation model for athletes based on the LVN-FS model was shown in Figure 4. The process of the fatigue muscle strength estimation model for athletes included the following steps. Firstly, the EMG signal data of athletes were acquired by EMG signal acquisition equipment. Then, the acquired data were preprocessed including filtering, noise reduction, and other operations. The features were extracted from the preprocessed data such

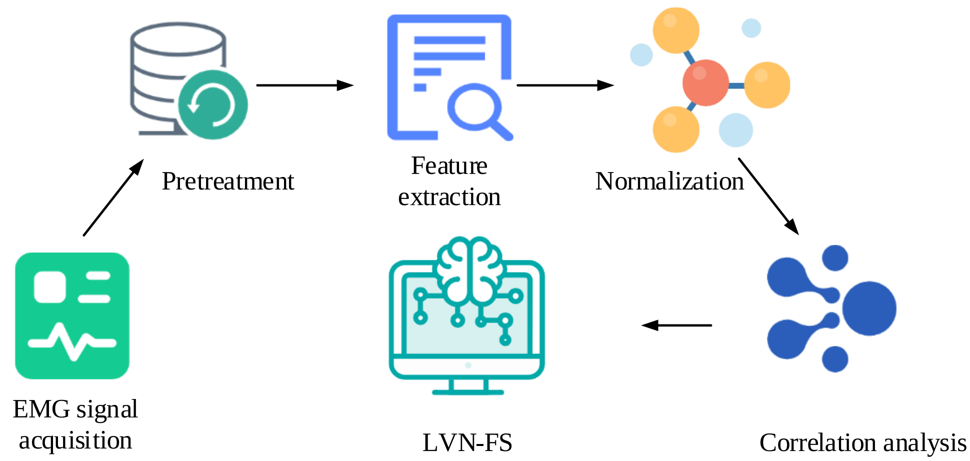

Figure 4. A fatigue muscle strength estimation model for athletes based on LVN-FS model.

as time-domain features, frequency-domain features, *etc*. followed by normalization of the extracted features to eliminate the differences between different athletes. Then, correlation analysis was carried out to find out the features related to fatigue muscle strength. Finally, fatigue muscle strength estimation was carried out by using the LVN-FS model, which could be used to achieve accurate estimation of fatigue muscle strength of athletes through feature selection and classifier training. In the construction process of the athlete fatigue muscle strength estimation model, the main data used was the athlete's electromyographic signal data, which was collected through electromyographic signal acquisition equipment.

Validation of constructed fatigue muscle strength estimation model

In the process of validating the model, other types of data were also used such as physiological indicators of athletes including heart rate, blood pressure, *etc*., and exercise performance data such as speed, strength, *etc*. Those data could help verify the accuracy and effectiveness of the model. At the same time, to ensure the generalization ability of the model, electromyographic signal data from different athletes, different sports events, and different training states were used for model validation. The experiments were carried out by using graphic processors (GPUs) and CPU processors with strong computational power to accelerate the training and inference process of the model. The Python programming language (https://www.python.org/) was mainly used and combined with deep learning frameworks, TensorFlow (https://www.tensorflow.org/) and PyTorch (https://pytorch.org/), for implementation. In addition, to better handle large-scale datasets, distributed computing, data parallelism, and other techniques were also used in the experimental process. Some common data processing and visualization libraries including NumPy (https://numpy.org/) and Pandas (https://pandas.pydata.org/) were also used in the specific implementation in order to pre-process and analyze the data. To verify the effectiveness of the LVN-FS model proposed in the study, the classical polynomial fitting model (POL) and the Laguerre (LET) model were experimentally used as comparison methods.

Results and discussion

EMG signal data acquisition and processing

The EMG signal acquisition from volunteer #1 was shown in Figure 5. Within the first 25 seconds, the maximum voluntary contraction force of the muscle force occurred, which indicated that the muscle was in a more tense

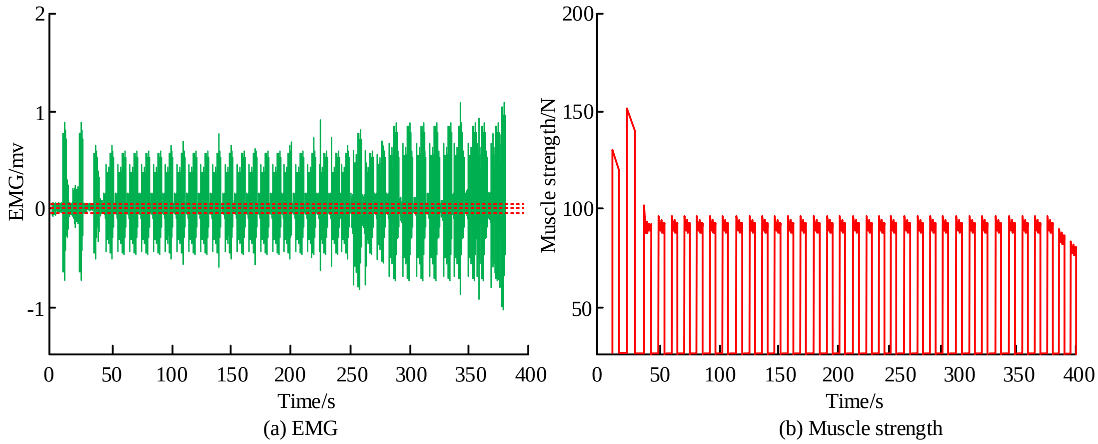

Figure 5. The collection of electromyographic signals from volunteer 1.

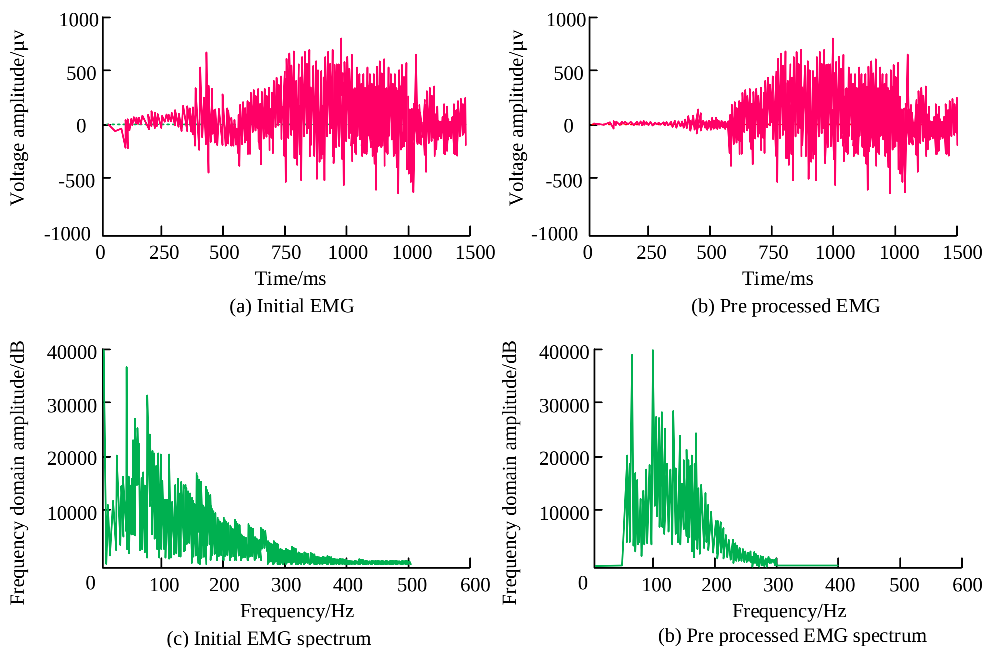

Figure 6. Preprocessing results of EMG.

state. Then, the size of the muscle force gradually changed to 70% of the maximum voluntary contraction force, which indicated that the muscle had started fatigue. After 260 seconds, the EMG showed obvious fluctuation, which indicated that the athlete's muscle force had gradually transitioned from a non-fatigue state to a fatigue state, and at the same time, the movement noise gradually increased. The results suggested that the pre-processing of EMG was very necessary to ensure the acquisition of accurate and reliable EMG signal data. The pre-processing results of EMG were shown in Figure 6. The baseline drift of the EMG signal was effectively suppressed after data preprocessing, which could be achieved by an effective filtering technique. After 50 - 300 Hz bandpass filtering, the low and high frequency components of the EMG signal were effectively removed, resulting in a clearer and more accurate signal. The series

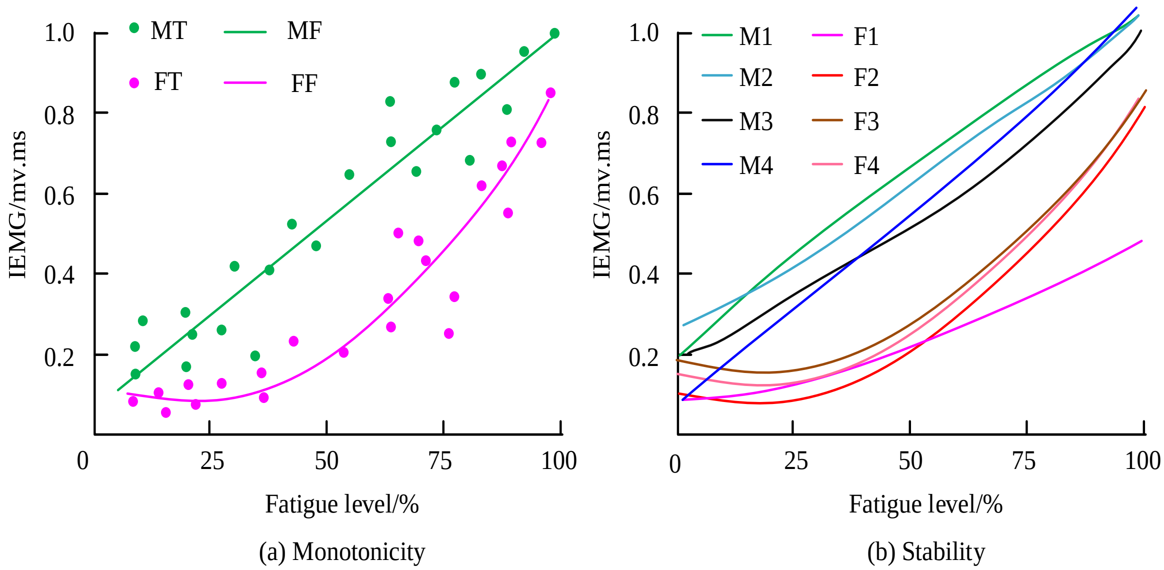

Figure 7. Evaluation results of partial time-domain features. MT and MF denote the measured calculated values and fitted curves of IEMG for male athletes, and FT and FF denote the measured calculated values and fitted curves of IEMG for female athletes, respectively. M1-4 represented the trend of IEMG test for four male athletes, and F1-4 represented the fitted curves of IEMG for four female athletes, respectively.

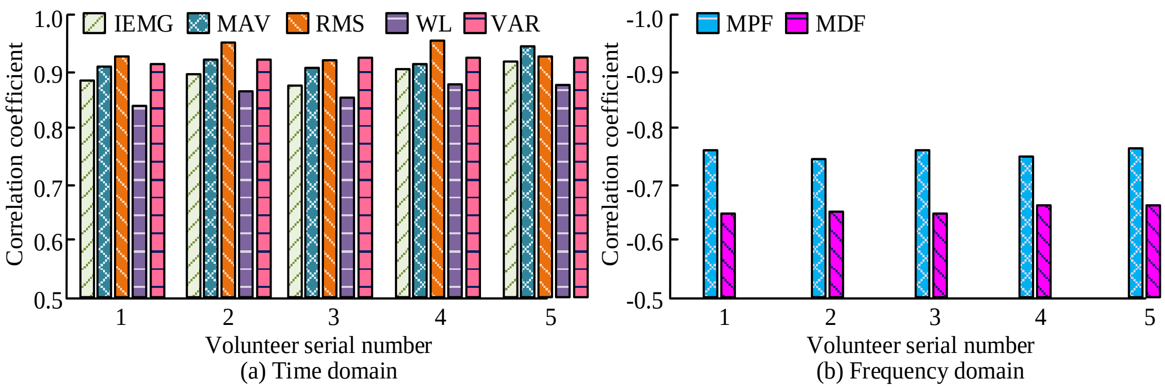

Figure 8. The correlation analysis results between different characteristic parameters of EMG and fatigue degree.

of preprocessing steps provided a more reliable and accurate data foundation for the subsequent analysis and interpretation of the EMG signal. The evaluation results of the time-domain feature IEMG were shown in Figure 7. The time-domain feature IEMG showed a monotonically increasing trend with the increase of fatigue (Figure 7a). Meanwhile, the time-domain features RMS, MAV, and WL had similar properties. The curves of the time-domain feature IEMG demonstrated a high degree of overlap and monotonicity consistent with the fitting effect in Figure 7a (Figure 7b). The monotonicity and stability of different characteristic parameters of EMG could be analyzed according to the same process described above. The results of the correlation analysis between different characteristic parameters of EMG and fatigue level were shown in Figure 8. The time-domain characteristic parameters of IEMG, MAV, RMS, WL, and VAR showed high positive correlations with the fatigue level with correlation coefficients of 0.876, 0.901, 0.908, 0.911, and

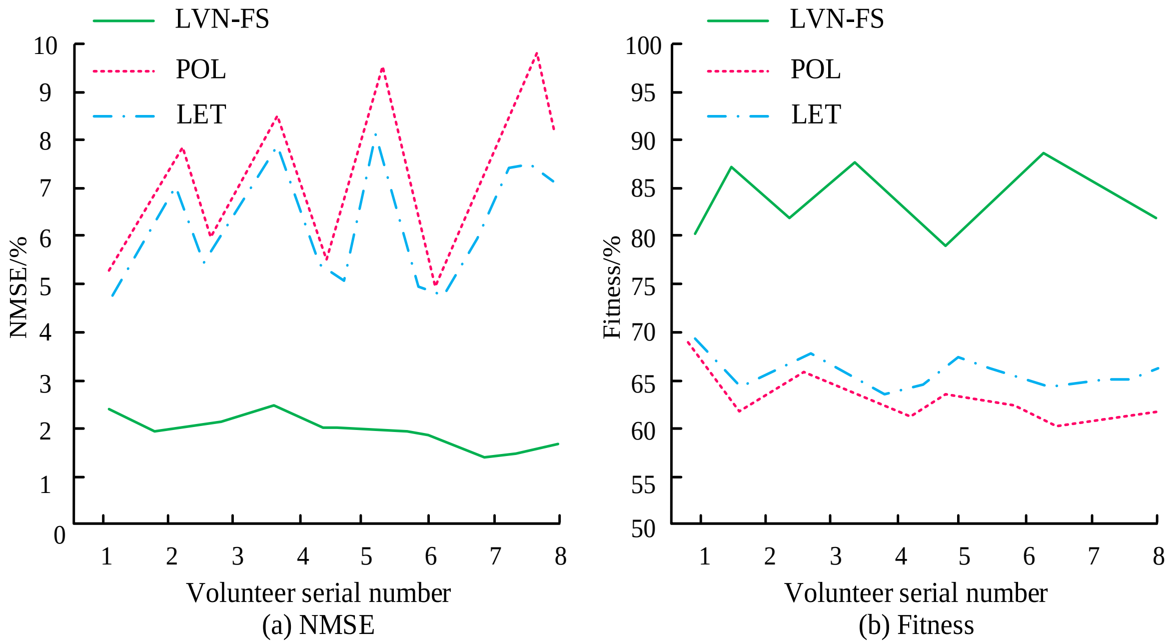

Figure 9. Test results of different models on the full pulse data of the radial muscle in volunteers.

0.898, respectively, which suggested that these time-domain characteristic parameters increased with the fatigue level, possibly reflecting the cumulative energy of the muscular activity and the activation of the muscles. The frequency domain parameters of MPF and MDF showed high negative correlation with the fatigue level with correlation coefficients of -0.766 and -0.663, respectively, which implied that the values of MPF and MDF decreased with the increase of fatigue level. The decreases of MPF that stood for the main frequency of the EMG signals and MDF that stood for the maximal power frequency might reflect the changes of the frequency distribution of EMG signals induced by muscle fatigue. The time-domain feature parameters showed a positive correlation with the degree of fatigue, whereas the frequency-domain feature parameters showed a negative correlation with the degree of fatigue. The analysis of these parameters could provide a quantitative indicator of the state of muscle fatigue, which was useful for assessing the degree of muscle fatigue and monitoring exercise performance.

Analysis of the application of models for estimating fatigue muscle strength in athletes

The test results of the different models on the full pulse data of the radial muscle of volunteers were shown in Figure 9. The error NMSE of the LVN-FS model was in the range of 1 - 4%, which was approximately 5% lower than that of the POL and LET models. The fitness of the LVN-FS model was in the range of 80 - 90%, which was approximately 21% improved compared to the POL and LET models. The results showed that the LVN-FS model had a significant improvement in both error and fitness with respect to the POL and LET models, which made it fitting the actual observed data more accurately and with a higher degree of fitting. The test results of different models in the fatigue stage were shown in Figure 10. For the prediction of muscle strength for different fatigue levels, the error of the LVN-FS model was in the range of 2 - 6%, which was smaller than that of the POL and LET models, and the degree of fit of the LVN-FS model was in the range of 70 - 90%, which was greater than that of both the POL and LET models. Therefore, the LVN-FS model was a better and more reliable

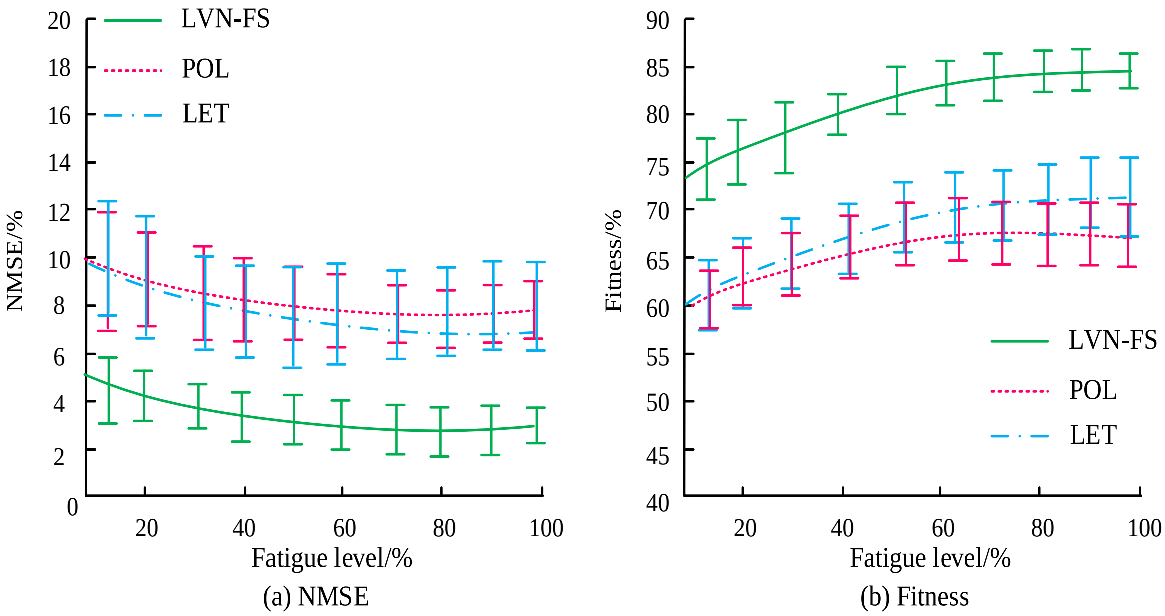

Figure 10. Test results of different models during fatigue stage.

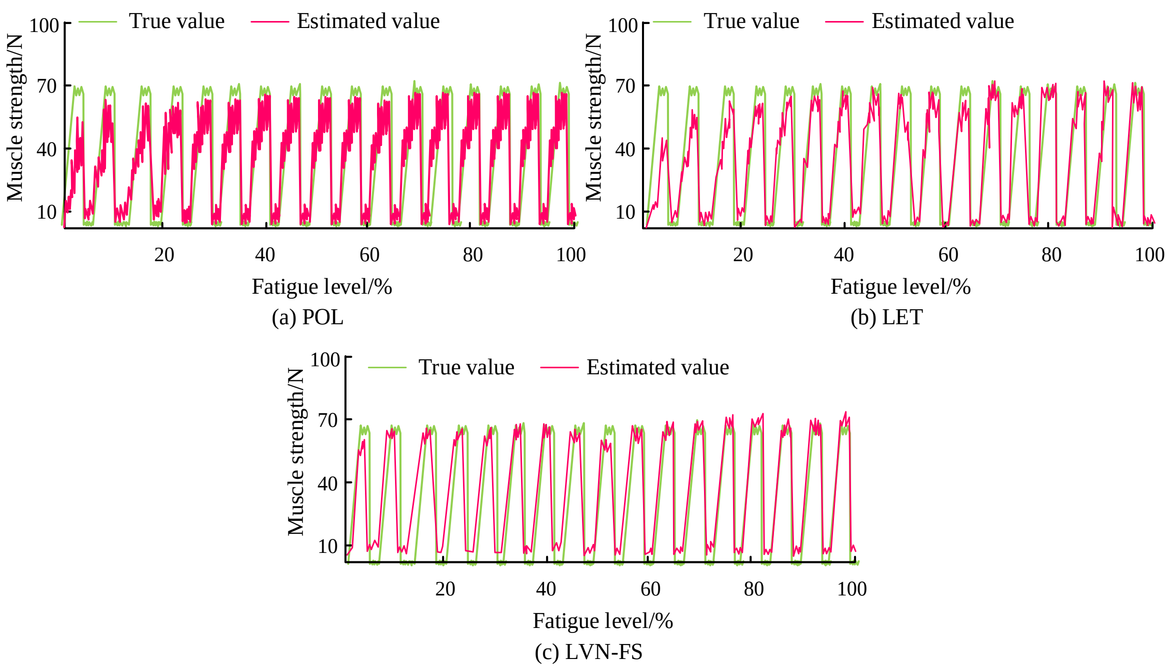

Figure 11. Muscle strength estimation using different models.

and valid model choice. The experimental results of different models for muscle force estimation were shown in Figure 11. The LVN-FS model's estimation of fatigue muscle force was closer to the real muscle force data than that of the POL and LET models. The results confirmed that the LVN-FS model had higher accuracy and reliability in estimating muscle force and was able to better capture the trend of fatigue muscle force and provide estimates closer to the real situation.

Conclusion

The study proposed a fatigue muscle force estimation model for athletes based on LVN-FS by input expansion and feature fusion on the basis of LVN model and combined feature selection and classifier training to achieve the estimation of fatigue muscle force of athletes. The results showed that the fatigue muscle strength estimation model for athletes based on the LVN-FS model had high accuracy and reliability and could more accurately fit the actual observed data with a higher degree of fitness. The model provided quantitative indicators for assessing athletes' fatigue status and monitoring sports performance, which could help to improve athletes' training effect and sports performance. This study only analyzed the EMG signals of the radial muscles of the athletes and did not consider the EMG signals of other muscles. Future studies could consider combining EMG signals from other muscles to improve the generalizability of the model.

References

1. Vasiljevas M, Damaševičius R, Maskeliūnas R. 2023. A human-adaptive model for user performance and fatigue evaluation during gaze-tracking tasks. Electron. 12(5):1130-1155.
2. Perpetuini D, Formenti D, Cardone D, Trecroci A, Rossi A, Credico A, *et al*. 2023. Can data-driven supervised machine learning approaches applied to infrared thermal imaging data estimate muscular activity and fatigue? Sensors. 23(2):832-848.
3. Kons RL, Orssatto LBR, Sakugawa RL, Junior JN. 2023. Effects of stretch-shortening cycle fatigue protocol on lower limb asymmetry and muscle soreness in judo athletes. Sports Biomech. 22(9):1079-1094.
4. Chen Q, Li Y, Yuan X. 2021. A hybrid method for muscle artifact removal from EEG signals. J Neurosci Meth. 353(1):109104-109113.
5. Schwartz C, Francois C, Benedicte D, Vincent B, Olivier C, Jean L. 2020. Normalizing gastrocnemius muscle EMG signal: An optimal set of maximum voluntary isometric contraction tests for young adults considering reproducibility. Gait Posture. 82(1):196-202.
6. Moissenet F, Tabard-Fougère A, Genevay S, Armand S. 2022. Normalization of a biarticular muscle EMG signal using a submaximal voluntary contraction: choice of the standardized isometric task for the rectus femoris, a pilot study. Gait Posture. 91(1):161-164.
7. Dideriksen J, Elias L, Zambalde E, Germer C, Molinari R, Negro F. 2021. Influence of central and peripheral motor unit properties on isometric muscle force entropy: A computer simulation study. J Biomech. 139(1):110866-110872.
8. Wang L, Zhang X, He Y, Wang Y, Zhong W, Mequanint K, *et al*. 2019. Ultralight conductive and elastic aerogel for skeletal muscle atrophy regeneration. Adv Funct Mater. 29(1):1806200-1806216.
9. Takenaka Y, Matsumoto H, Suzuki T, Sugawara K. 2023. Corticospinal excitability changes during muscle relaxation and contraction in motor imagery. Eur J Neurosci. 58(8):3810-3826.
10. Tang W, Wang A, Ramkumar S, Nair R. 2019. Signal identification system for developing Rehabilitative device using deep learning algorithms. Artif Intell Med. 102(1):101755-101763.
11. Li P, Yang X, Yin G, Guo J. 2020. Skeletal muscle fatigue state evaluation with ultrasound image entropy. Ultrason Imaging. 42(6):235-244.
12. Rakshit R, Xiang Y, Yang J. 2021. Functional muscle group- and sex-specific parameters for a three-compartment controller muscle fatigue model applied to isometric contractions. J Biomech. 127(1):110695-110701.
13. Wang Z, Zhao Y, He Y, Zhang J. 2021. Phase lag index-based graph attention networks for detecting driving fatigue. Rev Sci Instrum. 92(9):94105-94113.
14. Kim K, Sheng Z, Sharma N. 2019. Assessing FES-induced muscle fatigue using ultrasound to determine the inverse neuromuscular model for optimal FES input. J Acoust Soc Am. 145(3):1858-1858.
15. Villanueva A, Jang S, Stuerzlinger W, Ambike S, Ramani K. 2023. Advanced modelling method for quantifying cumulative subjective fatigue in mid-air interaction. Int J Hum-Comput St. 169(1):102931-102341.
16. Krishnamani DB, Pa K, Swaminathan R. 2020. Variational mode decomposition based differentiation of fatigue conditions in muscles using surface electromyography signals. IET Signal Process. 14(10):745-753.
17. Frey-Law LA, Schaffer M, Frank K. 2021. Muscle fatigue modelling: Solving for fatigue and recovery parameter values using fewer maximum effort assessments. Int J Ind Ergonom. 82(1):183104-183114.
18. Zhang W, Wang Q, Xu Z, Shang Y, Xu H. 2023. Development of a tractor operator-operation environment coupled biomechanical model and analysis of lower limb muscle fatigue. Int J Ind Ergonom. 93(1):1033407-103415.
19. Hamard R, Hug F, Kelp NY, Feigean R, Aeles J, Dick T. 2022. Inclusion of image-based in vivo experimental data into the Hill-type muscle model affects the estimation of individual force-sharing strategies during walking. J Biomech. 135(4):111033-111060.
20. Xu X, Cisewski-Kehe J, Davis AB, Fischer DA, Brewer JM. 2019. Modeling the echelle spectra continuum with alpha shapes and local regression fitting. Astron J. 157(6):243-259.
21. Yang B, Chen Y, Wang F, Cai Y. 2021. Trapping two types of Rayleigh particles simultaneously by a focused rotational elliptical Laguerre-Gaussian correlated Schell-model beam. J Quant Spectrosc Radiat Transf. 262(4):107518-107525.

22. Choudhuri S, Adeniye S, Sen A. 2023. Distribution alignment using complement entropy objective and adaptive consensus-based label refinement for partial domain adaptation. Artif Intell Appl. 1(1):43-51.
23. Hebbi C, Mamatha H. 2023. Comprehensive dataset building and recognition of isolated handwritten Kannada characters using machine learning models. Artif Intell Appl. 1(3):179-190.
24. Purohit J, Dave R. 2023. Leveraging deep learning techniques to obtain efficacious segmentation results. Archives of Advanced Engineering Science. 1(1):11-26.